Biochimie xxx (xxxx) xxx

Contents lists available at ScienceDirect

Biochimie

journal homepage: www.elsevier.com/locate/biochi

Unveiling the biodiversity of lipid species in *Corynebacteria*- characterization of the uncommon lipid families in *C. glutamicum* and pathogen *C. striatum* by mass spectrometry

Hay-Yan J. Wang [a, g, 1], Raju V.V. Tatituri [b, 1], Nicholas K. Goldner [c, 1], Gautam Dantas [c, d, e, f], Fong-Fu Hsu [a, *]

[a] *Mass Spectrometry Resource, Division of Endocrinology, Diabetes, Metabolism, and Lipid Research, Department of Medicine, Washington University School of Medicine, St. Louis, MO 63110, USA*
[b] *Division of Rheumatology, Immunology, and Allergy, Brigham and Women's Hospital, Harvard Medical School, 60 Fenwood Road, Boston, MA, 02115, USA*
[c] *The Edison Family Center for Genome Sciences, Washington University School of Medicine, St Louis, MO 63110, USA*
[d] *Department of Molecular Microbiology, Washington University School of Medicine, St Louis, MO 63110, USA*
[e] *Department of Pathology and Immunology, Washington University School of Medicine, St. Louis, MO, 63110, USA*
[f] *Department of Biomedical Engineering, Washington University in St Louis, St Louis, MO 63130, USA*
[g] *Department of Biological Sciences, National Sun Yat-Sen University, Kaohsiung, 80424, Taiwan*

ARTICLE INFO

Article history:
Received 1 April 2020
Received in revised form
21 June 2020
Accepted 3 July 2020
Available online xxx

Keywords:
Multiple stage linear ion-trap mass spectrometry
CDP-Diacylglycerol
Mycolic acid-containing PG
Microbial lipids
Lipidomics

ABSTRACT

Uncommon lipids in biotechnologically important *Corynebacterium glutamicum* and pathogen *Corynebacterium striatum* in genus *Corynebacterium* are isolated and identified by linear ion-trap multiple stage mass spectrometry (LIT MS^n) with high resolution mass measurement. We redefined several lipid structures that were previously mis-assigned or not defined, including cytidine diphosphate diacylglycerol (CDP-DAG), glucuronosyl diacylglycerol (GlcA-DAG), (α-D-mannopyranosyl)-(1 → 4)-(α-D-glucuronyl diacyglycerol (Man-GlcA-DAG), 1-mycolyl-2-acyl-phosphatidylglycerol (MA-PG), acyl trehalose monomycolate (acyl-TMM). We also report the structures of mycolic acid, phosphatidylglycerol, phosphatidylinositol, cardiolipin, trehalose dimycolate lipids in which many isomeric structures are present. The LIT MS^n approaches afford identification of the functional group, the fatty acid substituents and their regiospecificity in the molecules, revealing the biodiversities of the lipid species in two *Corynebacterium* strains that have played very different and important roles in human nutrition and health.

1. Introduction

The genus *Corynebacterium* currently has more than 110 validated species [1] and more than half of them are medically relevant [2]. Among them, *Corynebacterium striatum (C. striatum)* is known as an emerging opportunistic pathogen in patients with chronic diseases [3,4], and can colonize the skin much like *Staphylococcus aureus* (*S. aureus)* and has the ability to rapidly transition from susceptible to resistant to antibiotics including daptomycin [4–6]. The *Corynebacterium* genus also includes species that are biotechnologically relevant, for example, *C. glutamicum* is known to be one of the most important biotechnological workhorses for the production of many valuable chemicals [1,7].

The *Corynebacterium* and *Mycobacterium* genera are gram-positive bacteria belonging to the suborder Corynebacterineae, in which the complex cell envelope contains a great number of lipid classes in which several are known to contribute to the intrinsic resistance of these bacteria to many antibiotics and their success as pathogens. For example, mycolic acids have played crucial roles in the architecture of the cell envelope, and in mouse models, oxygenated mycolic acids are found to be necessary for virulence of *M. tuberculosis* [8]. Interestingly, while dispensability of corynomycolic acids for inhibition of phagolysosome maturation by pathogenic *Corynebacterium species such as C. diphtheriae* is independent of the presence or absence of mycolic acids, co-localization of corynomycolic acids in nonpathogenic C. glutamicum for inhibition of phagolysosome maturation is relatively fast [9].

* Corresponding author Box 8127, Washington University School of Medicine, 660 S Euclid, St. Louis, MO, 63110, USA.
E-mail address: fhsu@im.wustl.edu (F.-F. Hsu).
[1] These authors contribute equally.

https://doi.org/10.1016/j.biochi.2020.07.002
0300-9084/

Abbreviations

HRMS	high resolution mass spectrometry
ESI-MS	electrospray ionization-MS
LIT	linear ion-trap
CDP-DAG	cytidine diphosphate diacylglycerol
GlcA-DAG	glucuronosyl diacylglycerol
Man-GlcA-DAG	α-D-mannopyranosyl)-(1 → 4)-(α-D-glucuronyl diacyglycerol
MA	mycolic acid
PG	phosphatidylglycerol
PI	phosphatidylinositol
CL	cardiolipin
TMM	trehalose monomycolate
acyl-TMM	6-O-acyl trehalose monomycolate
TDM	trehalose dimycolate
PIM	phosphatidylinositol mannoside
MA-PG	1-mycolyl-2-acyl phosphatidylglycerol (or 1-mycolyl-2-acyl-sn-*glycero*-3-*phosphoglycerol)*

The lipids in the cell envelopes of Corynebacterineae are complex. For example, Yague and coworkers found unusual fatty acyl moiety in the phospholipid composition in several clinically relevant *Corynebacterium* species, applying various mass spectrometric techniques, including FAB, ESI mass spectrometry and GC/MS [10]. Recently, Klatt and coworkers identified 28 lipid subclasses and more than 233 molecular species in *C. glutamicum* including new subclasses of acylated/acetylated trehalose mono/dicorynomycolic acids, using high-resolution LC/MS/MS coupled with mass spectral library searches with MS-DIAL tool [11].

In an attempt to a better understanding the roles of lipids may play in the virulence of the pathogenic and drug resistant *C. striatum* [5] and in the lipid transport of the non-pathogenic and biotechnologically important *C. glutamicum*, we apply multiple stage tandem mass spectrometry (LIT MS^n) combined with high resolution mass spectrometry to conduct a thorough study of the lipid structures found in these two *Corynebacterium* strains that have significant differences in their roles in human welfare. We found that they all contain the lipid classes commonly seen in the *Corynebacterium* genus as reported previously. We also found several lipid families that have not been reported or their structures in which the regiospecificity of fatty acyl chain have been reversed. Here, we report our findings.

2. Method and materials

2.1. Growth and lipid extraction

C. striatum WT were grown in the presence of cation-adjusted MHB (BBL Mueller-Hinton II broth) with supplemental calcium added to reach 50 mg/L for 24 h at 37 °C with agitation in 10-mL tubes with 5 mL of culture. Liquid cultures were spun down to form a cell pellet, and whole-cell lipids were extracted using the Bligh-Dyer method [12]. Briefly, wet cells were suspended in 3.8 mL 1:2:0.8 chloroform:methanol:0.9% NaCl solution (v/v/v) in a 10 mL glass centrifuge tube, and were sonicated with a 10 mm sonicator probe tip (Q500 Sonicator) at 20% amplitude using a program of 1 s on, 1 s off for 2.5 min. This is followed by addition of 1 mL of chloroform and 1 mL of 0.9% NaCl, and vortexed for another 2 min. After centrifugation at 1200 rpm for 5 min, the bottom organic layer was removed by a glass Pasteur pipette. The upper layer was re-extracted twice with 3.8 mL chloroform and the pooled lipid extracts were dried under a nitrogen stream and stored at − 20 °C until use.

C. glutamicum ATCC 13032 (the wild-type strain, referred to as *C. glutamicum* for the remainder of the text) was grown in Luria–Bertani broth (Difco) at 37 °C, with kanamycin at a concentration of 25 μg/mL. Samples for lipid analyses were prepared by harvesting cells grown on BHIS for 9 h up to an $A_{600\ nm}$ of 7–8. Cells were harvested by centrifugation, followed by saline washing and freeze drying. Lipids were initially extracted from 6 g of dry C. glutamicum cells according to the procedures of Dobson et al. as described previously [13].

2.2. Preparative HPLC isolation of lipid species

Preparative HPLC experiments were carried out using a Thermo Scientific (San Jose, CA) TSQ Vantage mass spectrometer with Thermo Accela UPLC operated by Xcalibur software. Separation of lipid was achieved by a Supelco 100 × 2.1 mm (2.7 μ particle size) Ascentis C-8 column at a flow rate of 260 μl/min. The mobile phase contained 10 mM ammonium formate (pH 5.0) both in acetonitrile-water (60:40, v/v) (solvent A), and in 2-propanol-acetonitrile (90:10, v/v) (solvent B). A gradient elution in the following manner was applied: 68% A, 0–1.5 min; 68–55% A, 1.5–4 min; 55–48% A, 4–5 min; 48–42% A, 5–8 min; 42–34% A, 8–11 min; 34–30% A, 11–14 min; 30–25% A, 14–18 min; 25–3% A, 18–23 min; 3–0% A, 25–30 min; 0% A, 30–35 min; 68% A, 35–40 min. During fractionation, ~95% of the lipid was sent to a fraction collector, and a small percentage (5%) of the lipid was sent to the mass spectrometer via a tee for LC/MS analysis, where the ESI/MS scans were set at 2 s/scan (scan range: *m/z* 400 to 2500). After completion, the reconstructed ion chromatograms (RICs) from LC/MS runs in the negative-ion (Figure s1) and positive-ion (Figure s2) modes (two separated injections) were constructed (see supplemental materials Figures s1 and s2) to build the retention times of the various lipid classes. Fractions containing the different lipid classes were further subjected to high resolution LIT MS^n for structural identification. Both positive/negative ion LC/MS runs were performed, providing complementary information for comprehensive screening the various lipid classes in the whole extract. For example, TAG was not detected in the negative ion mode, but can be easily detected in the positive ion mode as the NH_4^+adduct ions (the $[M + NH4]^+$ ion formation is due to the presence of ammonium formate in mobile phase A and B), while mycolic acid (MA) was readily detectable in the negative-ion mode as $[M - H]^-$ ions, but cannot be well detected in the positive ion mode. In addition, for the lipid classes that are detectable in both positive/negative ion modes, the $[M + H]^+$, $[M + NH_4]^+$ and $[M+ Na]^+$ ions seen in the positive ion mode can be matched by the corresponding $[M - H]^-$ and $[M - HCO_2]^-$ ions formed in the negative ion mode to confirm the lipid species. The RIC plots (Figure s1 and s2), which provide the HPLC elution time for the various lipid classes can serve as an index for the collected fractions that can be further analyzed by other analytical means for further structure characterization.

2.3. Mass spectrometry

High resolution (R = 100,000 at m/z 400) LIT MS^n experiments were performed on a Thermo LTQ Orbitrap Velos. Lipid fractions from *C. striatum* and *C. glutamicum* collected from HPLC separation were dissolved in methanol, and was continually infused (2 μL/min) into the ESI source, where the skimmer was set at ground potential, the electrospray needle was set at 4.5 kV, and temperature of the heated capillary was 300 °C. The automatic gain control of the ion trap was set to 5×10^4, with a maximum injection time of 200 ms. Helium was used as the buffer and collision gas at a pressure of

Please cite this article as: H.-Y.J. Wang et al., Unveiling the biodiversity of lipid species in *Corynebacteria*- characterization of the uncommon lipid families in *C. glutamicum* and pathogen *C. striatum* by mass spectrometry, Biochimie, https://doi.org/10.1016/j.biochi.2020.07.002

1×10^{-3} mbar (0.75 mTorr). The MS^n experiments were carried out with an optimized relative collision energy ranging from 30 to 40% and with an activation q value at 0.25, and the activation time at 10 ms. Mass spectra were accumulated in the profile mode, typically for 3–10 min for MS^n (n = 2, 3, 4, and 5) spectra.

2.4. Nomenclatures

Mycolic acids (R_1-CH(OH)-CH(R_2)-COOH) consist of a meromycolic chain (R_1CH) (the part from the R_1 terminal to the β-hydroxy carbon) and an α-alkyl (R_2) branch. To abbreviate, the previous designation "R_1CHO/$R_2CH_2CO_2H$-MA" ("meromycolate branch/the rest remaining part of the molecule that contains the shorter R_2 group-mycolic acid") was adopted [14]. This designation also reflects the fact that upon subjected to CID in the negative ion mode, the mycolic acid $[M - H]^-$ ions undergo β cleavage to form $R_2CH_2CO_2^-$ ions by eliminating the meromycolate branch as an aldehyde. Therefore, for example, 2-tetradecyl-3-hydroxy-octadecanoic acid which contains a C_{16}-meromycolate chain and a C_{14} α-branch (i.e., $R_1 = C_{15}H_{31}$, $R_2 = C_{14}H_{29}$), is designated as 16:0/16:0-MA. The mycolic acids with unsaturated bond(s) such as 2-tetradecyl-3-hydroxy-eicosenoic acid and 2-tetradecenyl-3-hydroxy-eicosanoic acid are designated as 18:1/16:0-MA and 18:0/16:1-MA, respectively. Thus, designation of 18:1/16:0-MA signifies that the molecule contains an unsaturated 18:1-meromycolate chain and an α-alkyl ($C_{14}H_{29}$) group (i.e., $R_1 = C_{17}H_{33}$, $R_2 = C_{14}H_{29}$); while 18:0/16:1-MA signifies that the molecule consists of a 18:0-meromycolate chain and an unsaturated α-$C_{14}H_{27}$ group ($R_1 = C_{17}H_{35}$, $R_2 = C_{14}H_{27}$). Same designation is also applied to the mycolic acid containing lipids such as 6-acyl trehalose monomycolate (acyl-TMM), trehalose dimycolate (TDM), and mycolic acid containing PG. For example, (16:0/16:0) MA/18:1-PG signifies that the molecule consists of a (16:0/16:0)-MA at sn-1, and a 18:1-FA at sn-2 of the PG molecule.

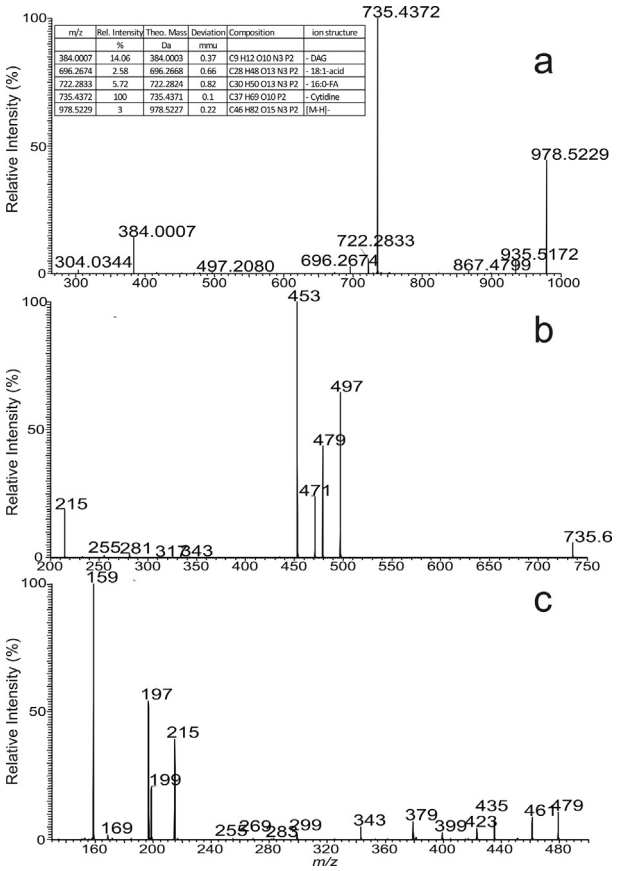

m/z	Rel. Intensity %	Theo. Mass Da	Deviation mmu	Composition	ion structure
384.0007	14.06	384.0003	0.37	C9 H12 O10 N3 P2	- DAG
696.2674	2.58	696.2668	0.66	C28 H48 O13 N3 P2	- 18:1-acid
722.2833	5.72	722.2824	0.82	C30 H50 O13 N3 P2	- 16:0-FA
735.4372	100	735.4371	0.1	C37 H69 O10 P2	- Cytidine
978.5229	3	978.5227	0.22	C46 H82 O15 N3 P2	[M-H]-

Fig. 1. The high-resolution MS^2 spectrum of the ion of *m/z* 978.5 (a), unit resolution MS^3 spectrum of *m/z* 735 (978 → 735) (b), and MS^4 spectrum of *m/z* 479 (978 → 735 → 479) (c). The inset table in (a) showed the deduced elemental compositions and the proposed ion structures.

3. Results and discussion

3.1. Characterization of cytidine diphosphate diacylglycerol (CDP-DAG) from C. striatum

CDP-DAG is a liponucleotide intermediate known to play an essential role in the biosynthesis of many complex glycerolipids via CDP-DAG pathway [15]. Although CDP-DAG can be found in eukaryotic and prokaryotic organisms, structural characterization of this lipid by mass spectrometry has not been well described. The LIT MS^n approaches toward characterization of this molecule found in Corynebacteria are described below.

In the negative ion mode, an $[M - H]^-$ ion was found at *m/z* 978.5, consistent with the observation of the corresponding $[M + H]^+$ ion at *m/z* 980.5 in the positive ion mode (Data not shown). High resolution mass measurement on the $[M - H]^-$ ion yielded *m/z* 978.5228, which led to an elemental composition of C46H82O15N3P2 (calculated *m/z*: 978.5227). The high-resolution CID MS^2 spectrum of the ion of *m/z* 978.5 (Fig. 1) contained the prominent ion at *m/z* 735.4372, representing a diacylglycero dehydrapyrophosphate anion arising from loss of a cytidine residue (Scheme 1a), together with the ion of *m/z* 384.0007, arising from loss of a 18:1/16:0-diacylglycerol (Scheme 1b). The presence of 18:1/16:0-DAG moiety is consistent with the observation of ions of *m/z* 722.2833 and 696.2674 arising from losses of 16:0- and 18:1-FA substituents, respectively, and in agreement with elemental compositions of the fragment ions extracted by HR mass measurements (Table 1). The ion of *m/z* 722 (loss of 16:0-FA) is more abundant than the ion of *m/z* 696 (loss of 18:1-FA), indicating that the 16:0- and 18:1-FA moieties are located at sn-2 and sn-1 of the glycerol backbone, respectively [16]. The above results led to assign the CDP-18:1/16:0-DAG structure. To further confirm the structure assignment, the ion of *m/z* 735 was further subjected to MS^3 (978 → 735; Fig. 1b), which resulted in ions of *m/z* 497 and 479, due to loss of 16:0-FA substituent as a ketene and an acid respectively, and ions of *m/z* 471 and 453, due to the analogous losses of the 18:1-FA moiety. The spectrum also contained the ion of *m/z* 215, arising from losses of both the 16:0- and 18:1-FA residues, along with ions of *m/z* 255 and 281, representing 16:0-, and 18:1-carboxylate anions, respectively. These later ions observed in the MS^3 spectra further confirm the identity of the fatty acid substituents of the molecule. The more abundant ion of *m/z* 453 (loss of 18:1-FA) than *m/z* 479 (loss of 16:0-FA) as seen in Fig. 1b is also in agreement with the observation of more prominent ion of *m/z* 497 (loss of 16:0-ketene) than 471 (loss of 18:1-ketene), indicating that the 18:1-, and 16:0-FA substituents are located at sn-2 and sn-1 of the glycerol backbone, respectively [17]. This assignment is consistent with the notion that loss the fatty acid moiety in glycerophospholipids involves the α-H of the neighboring fatty acid substituent in which the α-H of the FA at sn-2 is more labile, leading to more facile loss of the 18:1-FA substituent at sn-1. The more labile α-H of the 16:0-FA at sn-2 also facilitate its loss as a 16:0-ketene to *m/z* 497, which becomes more abundant than the ion of *m/z* 471 arising from the similar loss of 18:1-ketene at sn-1 [17].

Further fragmentation of the ion of *m/z* 479 (978 → 735 → 479; Fig. 1c) gave rise to ions of *m/z* 215 and 197, arising from loss of the remaining 18:1-FA as a ketene and an acid, respectively, along with the ion of *m/z* 159, representing a dehydrated pyrophosphate. The

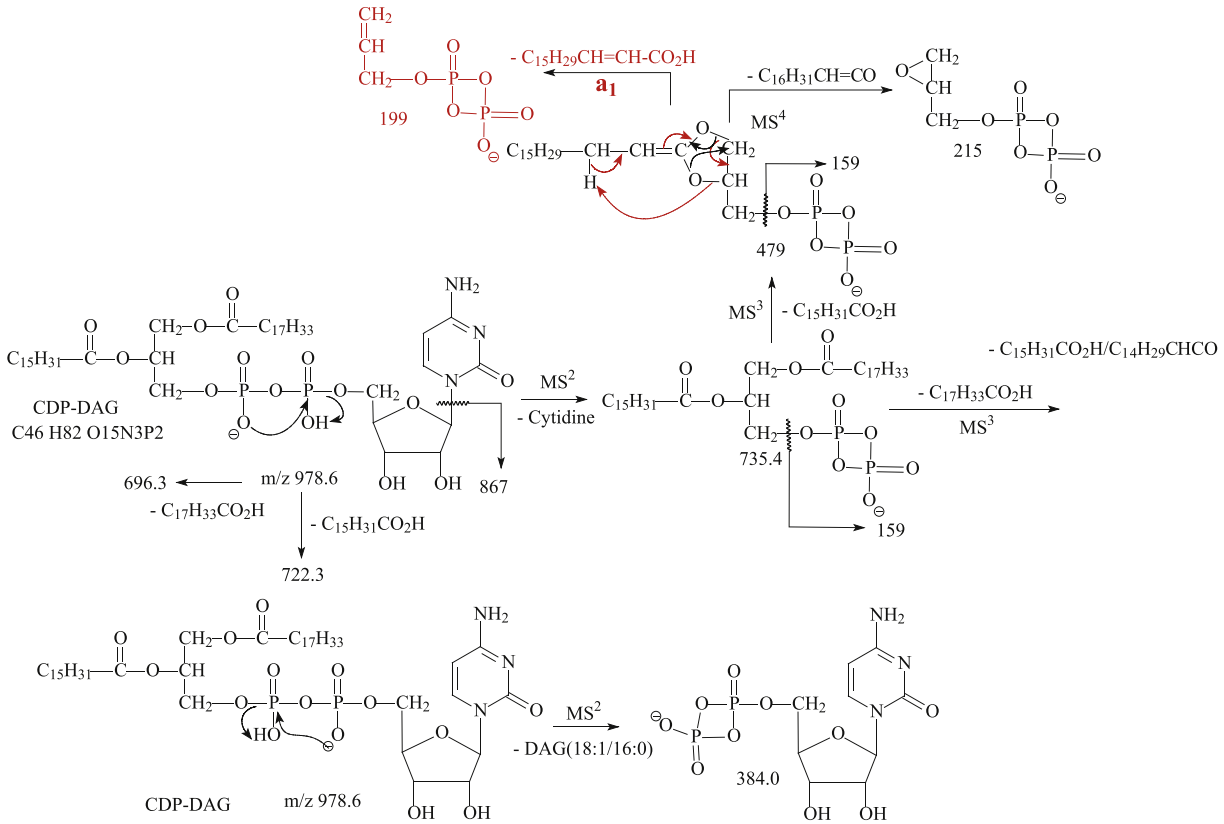

Scheme 1. The proposed fragmentation pathways of the [M - H]⁻ ions of the 18:1/16:0-CDP DAG at m/z 978. The cleavage of the O-P bonds led to formation of the dehydradiphosphate species of m/z 735 (a), and m/z 384 (b) that readily define the structure (see text for detail).

Table 1
High resolution MS^2 spectrum of the M − H]⁻ ion of CDP-18:1/16:0-DAG at *m/z* 978.5

m/z	Rel. Intensity	Theo. Mass	Deviation	Composition	ion structure
	%	Da	mDa		
304.0344	1.37	304.0340	0.37	C9 H11 O7 N3 P	- DAG - HPO3
384.0007	14.06	384.0003	0.37	C9 H12 O10 N3 P2	- DAG
453.1817	0.22	453.1813	0.46	C19H35 O8 P2	- Cytidine −18:1-acid
471.1924	0.14	471.1918	0.56	C19H37 O9 P2	- Cytidine −18:1-ketene
479.1974	0.17	479.1969	0.49	C21H37 O8 P2	- Cytidine −16:0-acid
497.2080	0.5	497.2075	0.56	C21H39 O9 P2	- Cytidine −16:0-ketene
696.2674	2.58	696.2668	0.66	C28H48 O13 N3 P2	- 18:1-acid
722.2833	5.72	722.2824	0.82	C30H50 O13 N3 P2	- 16:0-FA
735.4372	100	735.4371	0.1	C37H69 O10 P2	- Cytidine
740.2934	0.3	740.2930	0.41	C30H52 O14 N3 P2	−16:0-ketene
867.4799	0.96	867.4794	0.54	C42H77 O14 P2	-Cytosine
935.5172	5.21	935.5169	0.33	C45H81 O14 N2 P2	- HN=C=O
978.5229	3	978.5227	0.22	C46H82 O15 N3 P2	[M − H]⁻

spectrum also contained the ion of *m/z* 199, arising from loss of 16:0-FA as an α,β-unsaturated FA (loss as 16:1-FA) (Scheme 1a, route a_1). This unique loss of FA as an α,β-unsaturated FA species further confirms that the 16:0-FA is located at sn-2 of the glycerol backbone [18].

3.2. Characterization of glucuronosyl diacylglycerol (GlcA-DAG) and (α-D-mannopyranosyl)-(1 → 4)-(α-D-glucuronyl diacyglycerol (Man-GlcA-DAG) from C. striatum and C. glutamicum

GlcA-DAG is a major lipid family found in the genus of pseudomonas and was the first anionic glycolipid found in gram-negative bacteria [19,20]. Wolucka and coworkers established the structures of GlcA-DAG found in *Mycobacterium smegmatis* using NMR and GC/MS and FAB mass spectrometry [21]. Both GlcA-DAG and Man-GlcA-DAG lipids were reported in *C. glutamicum* cells and the major species were falsely reported as GlcA 16:0/18:1-DAG and ManGlcA 16:0/18:1-DAG [11,13].

To redefine the structure, we first applied high resolution negative ion ESI-MS mass measurement on the lipid family as the [M − H]⁻ ions, which showed the predominated ion of *m/z* 769.5471 corresponding to a C43H77O11 (calculated *m/z*: 769.5464) elemental composition (Table s1e). High resolution MS^2 on the ion of *m/z* 769.5 (Fig. 2a) gave rise to ions of *m/z* 531 and 513, arising from loss of 16:0-FA substituent as a ketene and an acid, respectively, together with ions of *m/z* 505 and 487 arising from the analogous losses of the 18:1-FA substituent (Table 2a) (Scheme 2a). The ion of *m/z* 531 (loss of 16:0-ketene) is more abundant than the

Please cite this article as: H.-Y.J. Wang et al., Unveiling the biodiversity of lipid species in *Corynebacteria*- characterization of the uncommon lipid families in *C. glutamicum* and pathogen *C. striatum* by mass spectrometry, Biochimie, https://doi.org/10.1016/j.biochi.2020.07.002

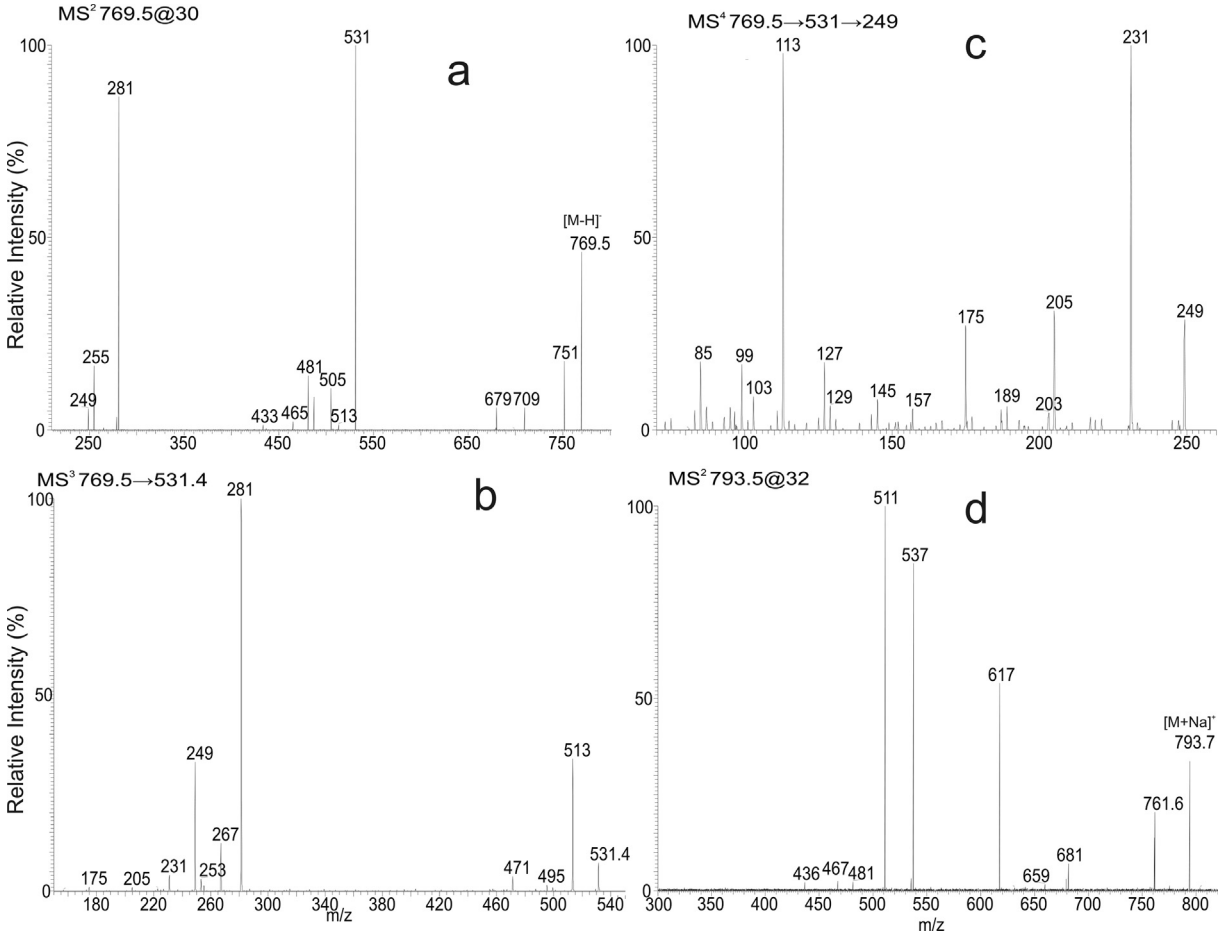

Fig. 2. The high-resolution MS^2 spectrum of the ion of *m/z* 769.5 (a), its MS^3 spectrum of the ion of *m/z* 531 (769 → 531) (b), and MS^3 spectrum of the ion of *m/z* 249 (769 → 531 → 249) (c). Panel (d) shows the MS^2 spectrum of the corresponding $[M + Na]^+$ ion at *m/z* 793.5, which also contains informative ions for structure assignment (see text for details).

ion of *m/z* 505 (loss of 18:1-ketene) indicating that the 16:0- and 18:1-FA substituents are respectively located at sn-2 and sn-1 [16]. This is also consistent with the notion that the ion of *m/z* 487 (loss of 18:1-FA) is more abundant than the ion of *m/z* 513 (loss of 16:0-FA) [17]. The spectrum also contained ions of *m/z* 255 (16:0-carboxylate) and 281 (18:1-carboxylate), consistent with the presence of 16:0- and 18:1-FA substituents in the molecule.

Further dissociation of the ion of *m/z* 531 (769 → 531) (Fig. 2b) yielded ions of *m/z* 267 and 249 arising from losses of 18:1-FA as a ketene and an acid, respectively, along with ion of *m/z* 281, representing a 18:1-carboxylate anion. The MS^4 spectrum of the ion of *m/z* 249 (769 → 531 →249) (Fig. 2c) contained ions of *m/z* 205 (loss of CO_2) and 175 (loss of [glycerol − H_2O]), 113 (175 − [H_2O + CO_2]) further support the presence of the GlcA-DAG moiety in the molecule (Scheme 2a). The above fragmentation processes were also supported by the HR mass measurements of fragment ions in the HCD MS^2 spectrum, in which the elemental compositions of the ions match the proposed ion structures (Table 2b). Taken together, these results point to the presence of a GlcA 18:1/16:0-DAG structure.

Table 2a
High resolution CID MS^2 spectrum of the $[M - H]^-$ ion of 18:1/16:0-DAGluA at *m/z* 769.54

m/z	Rel. Intensity	Theo. Mass	Deviation	Composition	ion structure
Da	%	Da	mDa		
231.0519	0.29	231.0510	0.92	C9 H11 O7	- (16:0-FA+18:0-FA)
249.0624	6.35	249.0616	0.86	C9 H13 O8	-(16:0-ketene+18:0-FA)
255.2338	25.05	255.2330	0.86	C16H31 O2	$C_{15}H_{31}CO_2^-$
281.2486	75.23	281.2486	0.01	C18H33 O2	$C_{17}H_{33}CO_2^-$
469.2808	0.62	469.2807	0.13	C25H41 O8	- 18:1-FA - H2O
487.2913	16.41	487.2913	0.07	C25H43 O9	- 18:1-acid
495.2964	0.61	495.2963	0.04	C27H43 O8	- 16:0-FA - H2O
505.3018	24.3	505.3018	0.01	C25H45 O10	- 18:1-ketene
513.3071	18.52	513.3069	0.15	C27H45 O9	- 16:0-FA
531.3176	100	531.3175	0.14	C27H47 O10	−16:0-ketene
709.5262	9.47	709.5260	0.18	C41H73 O9	- C2H4O2
751.5368	35.92	751.5366	0.23	C43H75 O10	- H2O
769.5474	41.09	769.5471	0.3	C43H77 O11	$[M - H]^-$

Please cite this article as: H.-Y.J. Wang et al., Unveiling the biodiversity of lipid species in *Corynebacteria*- characterization of the uncommon lipid families in *C. glutamicum* and pathogen *C. striatum* by mass spectrometry, Biochimie, https://doi.org/10.1016/j.biochi.2020.07.002

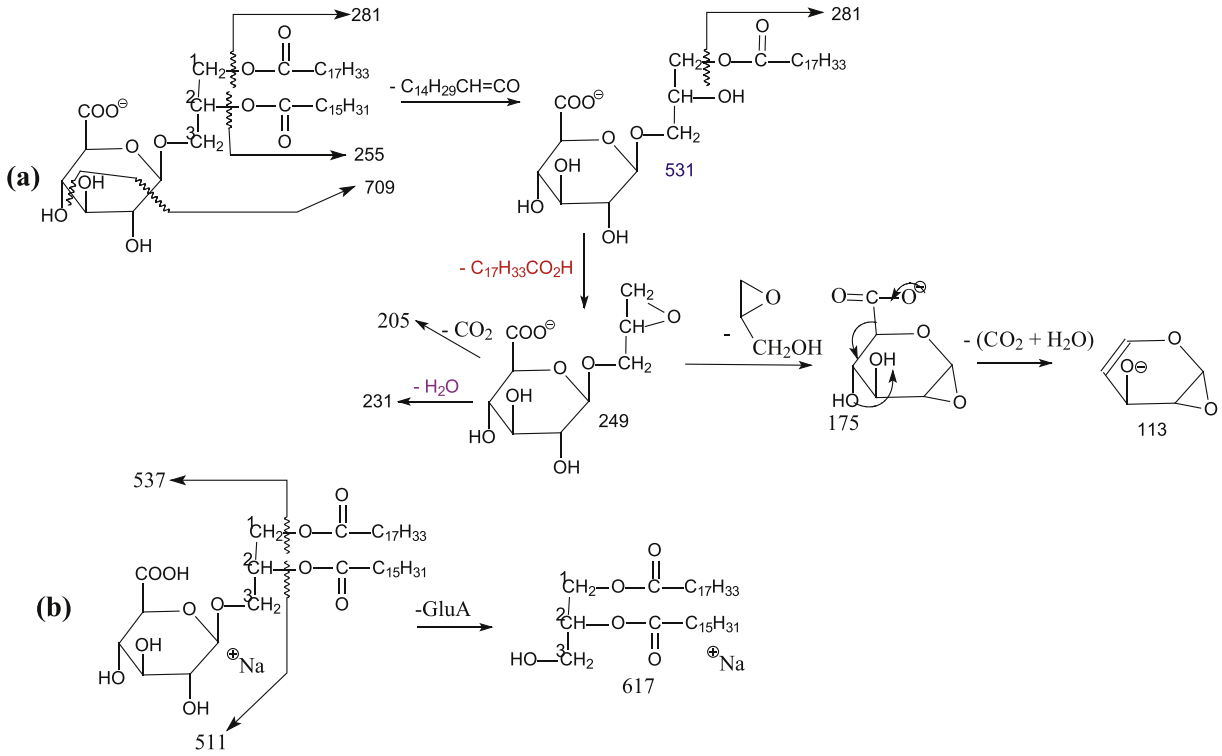

Scheme 2. The proposed fragmentation processes of 18:1/16:0-GlcA DAG in the $[M - H]^-$ ion (a), and in the $[M + Na]^+$ (b) forms.

Table 2b
High resolution HCD MS^2 spectrum of the $[M - H]^-$ ion of 18:1/16:0-DAGluA at *m/z* 769.54

m/z	Rel. Intensity	Theo. Mass	Deviation	Composition	structure assignment
	%	Da	mDa		
113.0252	31.00	113.0244	0.75	C5 H5 O3	$GluA^-$-$2H_2O$ - CO_2
129.02	1.85	129.0193	0.7	C5 H5 O4	$GluA^-$-$2H_2O$-CO
157.0148	1.75	157.0142	0.57	C6 H5 O5	$GluA^-$-$2H_2O$
175.0253	5.99	175.0248	0.5	C6 H7 O6	$GluA^-$-H2O
193.0358	3.75	193.0354	0.4	C6 H9 O7	$GluA^-$
205.0721	2.14	205.0718	0.33	C8 H13 O6	249 - CO_2
231.0512	2.36	231.051	0.22	C9 H11 O7	- (16:0-FA+18:0-FA)
249.0617	11.89	249.0616	0.13	C9 H13 O8	-(16:0-ketene+18:0-FA)
255.233	57.88	255.233	0.06	C16H31 O2	$C_{15}H_{31}CO_2^-$
281.2486	100.00	281.2486	−0.01	C18H33 O2	$C_{17}H_{33}CO_2^-$
487.2914	3.72	487.2913	0.11	C25H43 O9	- 18:1-acid
505.3019	6.54	505.3018	0.11	C25H45 O10	- 18:1-ketene
513.3071	4.60	513.3069	0.22	C27H45 O9	- 16:0-FA
531.3177	22.00	531.3175	0.22	C27H47 O10	−16:0-ketene
709.5263	1.38	709.526	0.28	C41H73 O9	- C2H4O2
751.5369	2.58	751.5366	0.31	C43H75 O10	- H2O
769.5470	47.30	769.5471	−0.18	C43H77 O11	$[M - H]^-$

HR MS^2 on the corresponding $[M + Na]^+$ ion at *m/z* 793.5 in the positive ion mode (Fig. 2d), gave rise to ions of *m/z* 537 and 511 from loss of 16:0- and 18:1-FA substituents, respectively, along with ion of *m/z* 617 arising from loss of the GluA residue (see Table 2c and Scheme 2b for the elemental compositions and proposed ion structures). The ion of *m/z* 511 is more abundant than the ion of *m/z* 537, indicating that the 18:1- and 16:0- FA substituents are located at sn-1 and sn-2, respectively [17], and further established that the molecule is indeed a GlcA 18:1/16:0-DAG (Scheme 2b), rather than a GlcA 16:0/18:1-DAG as previously defined.

In the negative-ion mode, the lipid species belongs to the Man-GlcA-DAG family was seen at *m/z* 931.6006, representing a $[M - H]^-$ ion with an elemental composition of C49H87O16 (Calculated *m/z*: 931.6000). High resolution MS^2 on the ion of *m/z* 931.6 (Fig. 3a) yielded a prominent ion at *m/z* 751.5365 (Calculated *m/z*: 751.5366) arising from loss of a hexose residue (i.e. a mannose; C6H12O6, which is (1 → 4) attached to (α-D-glucuronyl diacyglycerol) [13] (Table 3), along with ions (ions in Fig. 3a that are not labeled) probably arising from the other isobaric precursors that entered the collision cell and underwent fragmentation silmultaneously. However, MS^3 on the ion of *m/z* 751.5 (931 → 751; Fig. 3b) gave rise to the predominated ion pair of *m/z* 513/495. arising from losses of 16:0-FA as a ketene and acid, respectively, along with the *m/z* 487/469 ion pair arising from the analogous losses of the 18:1-FA residue (Scheme 3). The former ion pair is more abundant than the latter, indicating that the 18:1- and 16:0-FA substituents are located at sn-1, and sn-2 of the glycerol backbone, respectively. The spectrum also contained ions of *m/z* 281 18:1- carboxylate anion) and

Please cite this article as: H.-Y.J. Wang et al., Unveiling the biodiversity of lipid species in *Corynebacteria*- characterization of the uncommon lipid families in *C. glutamicum* and pathogen *C. striatum* by mass spectrometry, Biochimie, https://doi.org/10.1016/j.biochi.2020.07.002

Table 2c
High resolution MS^2 spectrum of the $[M + Na]^+$ ion of 18:1/16:0-DAGluA at *m/z* 793.54

m/z	Rel. Intensity	Theo. Mass	Deviation	Composition	ion structure
	%	Da	mDa		
467.2979	2.85	467.2979	0.01	C24H44 O7 Na	- 18:1-acid - CO2
481.2774	1.89	481.2772	0.17	C24H42 O8 Na	- 18:1-acid - HCHO
511.2878	100.00	511.2878	0.05	C25H44 O9 Na	- 18:1-acid
537.3036	65.64	537.3034	0.16	C27H46 O9 Na	- 16:0-FA
617.5119	45.38	617.5115	0.31	C37H70 O5 Na	-GluA
761.5180	7.50	761.5174	0.61	C42H74 O10 Na	- CH3OH
793.5438	59.69	793.5436	0.18	C43H78 O11 Na	$[M+Na]^+$

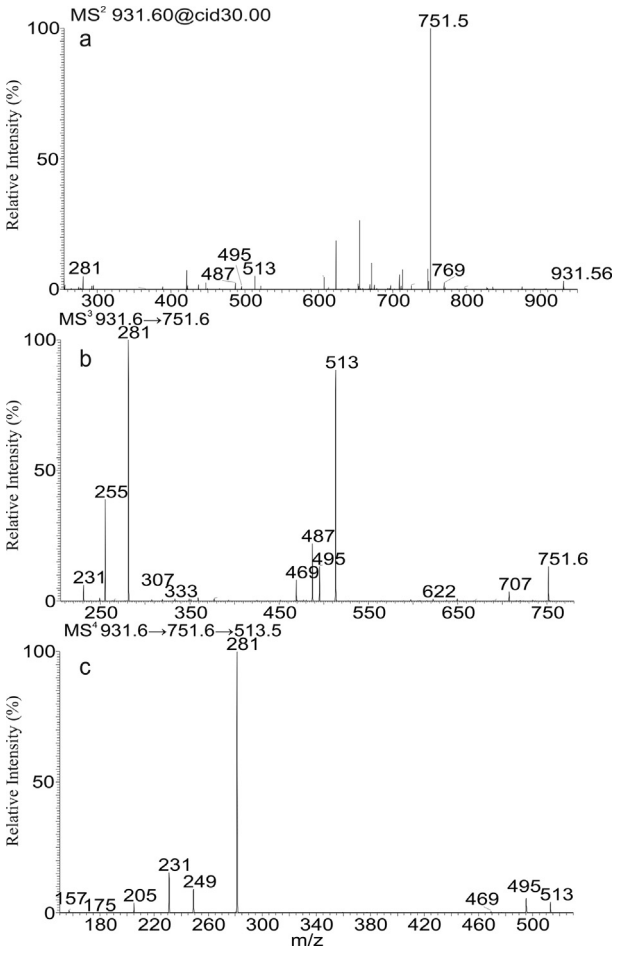

Fig. 3. The high resolution CID LIT MS^2 spectrum of the ion of *m/z* 931.6 (a), MS^3 spectrum of the ion of *m/z* 751.6 (931 → 751) (b), and MS^4 spectrum of the ion of *m/z* 513 (931 → 751 → 513) (c). Ions (not labeled) in Panel A are unrelated to the structure and are rejected in the consecutive MS^3 (Panel b) and MS^4 (c) spectra, which are readily applicable for structure identification.

255 (16:0-carbolylate anion), further support the presence of 18:1- and 16:0 substituents in this Man-GlcA-DAG family. The MS^4 spectrum of the ion of *m/z* 513 (931 → 751 → 513; Fig. 3c) contained the 249/231 ion pair arising from cleavage of the remaining 18:1-FA substituent as a ketene/acid, together with ions of 205 from further CO_2 loss from *m/z* 249. These results define the Man-GlcA-DAG (18:1/16:0) structure, which was, otherwise, reported as a Man-GlcA-DAG (16:0/18:1) previously [13].

3.3. Characterization of 1-mycolyl-2-acyl-phosphatidylglycerol (MA-PG) from C. glutamicum

High resolution ESI/MS revealed that six species in this lipid family were exclusively present in *C. glutamicum* (Table s1d). This lipid family was previously reported as PG-like lipids and their structures were not defined [11]. High resolution CID LIT MS^2 on the ion of *m/z* 961.7 (Fig. 4a), for example, yielded the major ion at *m/z* 495, corresponding to a 16:0/16:0-mycolic acid anion, together with the ion of *m/z* 465, arising from loss of 16:0/16:0-MA (Table 4). The spectrum also contained ions of *m/z* 723 and 705, arising from losses of the 16:0-FA substituent as a ketene and acid, respectively, together with ions of *m/z* 631 (723 − Glycerol) and 613 (705 − glycerol) arising from further loss of the glycerol residue of the glycerol head group [16]. The ions of *m/z* 723 (loss of 16:0-ketene) and 705 (loss of 16:0-Acid) are more abundant than ions of *m/z* 483 (loss of 32:0-MA ketene) and 465 (loss of 32:0-MA), indicating that the 16:0-FA, and 32:0-MA substituents are located at sn-2 and sn-1 of the glycerol backbone, respectively (see Scheme 4 for the proposed fragmentation processes).

To gain further insight into the structure, the ion of *m/z* 723 was further subjected to MS^3. The MS^3 spectrum of the ion of *m/z* 723 (961 → 723; Fig. 4b) contained the ions of *m/z* 631 arising from loss of glycerol and *m/z* 495, corresponding to a 16:0/16:0-MA anion. The results suggest that the ion of *m/z* 723 is likely formed from *m/z* 961 by loss of 16:0-FA substituent to form a lyso-PG possessing a mycolyl fatty acyl group at sn-1. Further dissociation of the ion of *m/z* 631 (961 → 723 → 631; Fig. 4c) gave rise to ion of *m/z* 495 by loss of a dehydrated glycerophophate (136 Da) residue. This specific neutral loss of 136 Da is a hallmark fragmentation process for

Table 3
High resolution MS^2 spectrum of the $[M - H]^-$ ion of Man-GlcA-DAG at *m/z* 931.

m/z	Rel. Intensity	Theo. Mass	Deviation	Composition	
Da	%	Da	mDa		ion structure
255.2337	4.22	255.2330	0.76	C16H31 O2	$C_{15}H_{31}CO_2^-$
281.2485	5.07	281.2486	−0.08	C18H33 O2	$C_{17}H_{33}CO_2^-$
495.2963	0.51	495.2963	−0.01	C27H43 O8	- ManGluA
513.3069	5.17	513.3069	0	C27H45 O9	- (ManGluA- H2O)
751.5365	100	751.5366	−0.11	C43H75 O10	-C6H12O6
769.5471	1.76	769.5471	−0.03	C43H77 O11	- C6H10O5
931.6006	3.27	931.6000	0.61	C49H87 O16	$[M - H]^-$

Please cite this article as: H.-Y.J. Wang et al., Unveiling the biodiversity of lipid species in *Corynebacteria*- characterization of the uncommon lipid families in *C. glutamicum* and pathogen *C. striatum* by mass spectrometry, Biochimie, https://doi.org/10.1016/j.biochi.2020.07.002

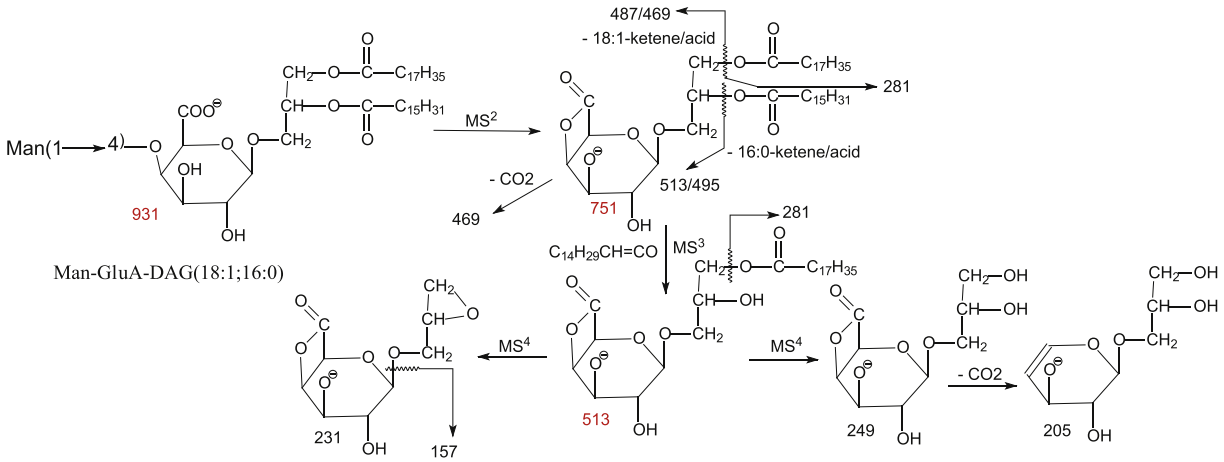

Scheme 3. The proposed fragmentation processes of the [M - H]⁻ ion of 18:1/16:0-Man-GluA DAG at m/z 931.

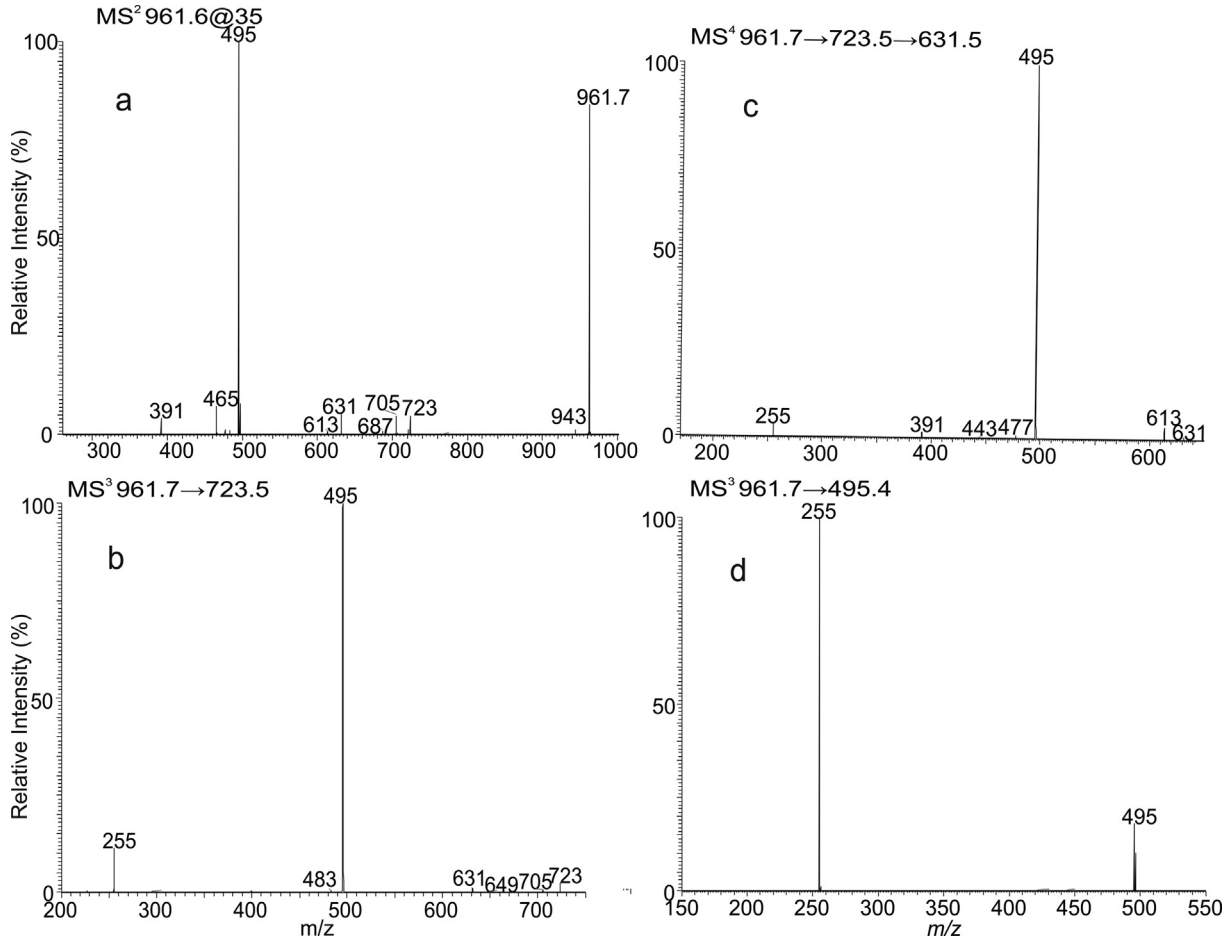

Fig. 4. The High resolution CID LIT MS^2 spectrum of the ion of *m/z* 961.7 (a), its MS^3 spectrum of the ion of *m/z* 723 (961 → 723) (b), MS^4 spectrum of ion of *m/z* 631 (961 → 723 → 631) (c), and MS^3 spectrum of the ion of *m/z* 495 (961 → 495)(d).

glycerophospholipids upon subjected to CID that results in the elimination of the head group and FA constituents [17,22], and further support the assigned 1-mycoly 2-acyl PG structure.

The MS^3 spectrum of the ion of *m/z* 495 (961 → 495; Fig. 4d), the MS^4 spectrum of the ion of *m/z* 495 (961 → 723 → 495; not shown), and the MS^5 spectrum of the ion of *m/z* 495 (961 → 723 → 631 → 495; not shown) are identical, and are all dominated by the ion of *m/z* 255. The spectra are also identical to the MS^2 spectrum of the [M – H]⁻ ion of 16:0/16:0-MA at *m/z* 495 (supplemental material Fig s1a). These results further support that the molecule possess a 16:0/16:0-MA residue. Taken together, the results confirm that the molecule is a 1-16:0/16:0-mycolyl, 2-palmitoyl phosphatidylglycerol. Similar LIT MS^n approaches led to assign the structures of the entire lipid family (Table s1d).

Please cite this article as: H.-Y.J. Wang et al., Unveiling the biodiversity of lipid species in *Corynebacteria*- characterization of the uncommon lipid families in *C. glutamicum* and pathogen *C. striatum* by mass spectrometry, Biochimie, https://doi.org/10.1016/j.biochi.2020.07.002

Table 4
High resolution MS^2 spectrum of the $[M - H]^-$ ion of 1-mycolyl-2-acyl-PG at *m/z* 961.

m/z	Rel. Intensity	Theo. Mass	Deviation	Composition	
Da	%	Da	mDa		ion structure
391.2254	4.12	391.2255	−0.13	C19H36 O6 P	465 - (gly - H2O)
465.2623	7.38	465.2623	0	C22H42 O8 P	loss of 14:0/18:0-MA (acid)
477.4677	1.46	477.4677	−0.05	C32H61 O2	495 - H2O
483.2728	1.17	483.2728	−0.03	C22H44 O9 P	loss of 14:0/18:0-MA (ketene)
495.4781	100	495.4783	−0.13	C32H63 O3	14:0/18:0-MA anion$^-$
631.4708	5.12	631.4708	0	C35H68 O7 P	705 - (gly - H2O)
687.4971	1.01	687.4970	0.12	C38H72 O8 P	705 - H2O
705.5076	4.79	705.5076	0.05	C38H74 O9 P	- 16:0(FA)
723.5182	4.88	723.5182	0.06	C38H76 O10 P	−16:0 (ketene)
943.7375	1.26	943.7373	0.24	C54H104 O10 P	- H2O
961.7480	2.8	961.7478	0.22	C54H106 O11 P	$[M - H]^-$

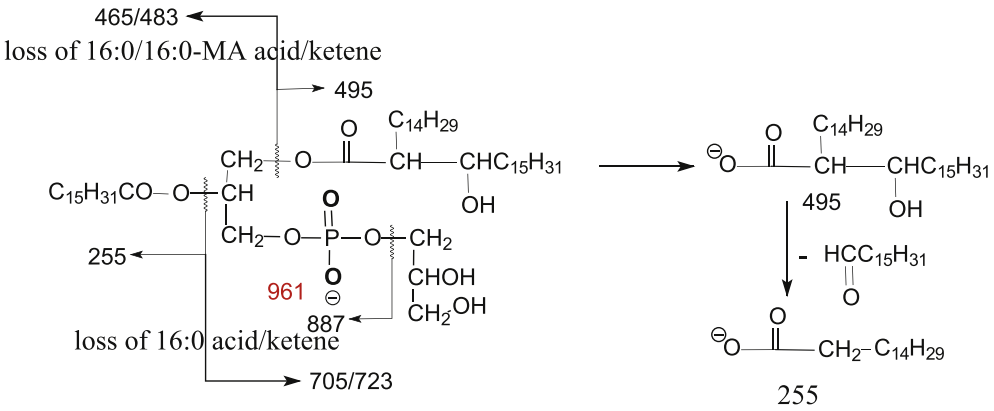

Scheme 4. The fragmentation pathways proposed for the [M - H]$^-$ ion of 1-(16:0/16:0) mycolyl 2-hexadecanoyl PG.

3.4. Characterization of acyl-TMM from C. glutamicum

In the positive ion mode, two sodiated acyl-TMM species were found at *m/z* 1081.8101 (calculated C60H114 O14 Na: 1081.8101 Da) and 1107.8253 (calculated C62H116 O14 Na: 1107.8257 Da), consistent with the observation of the $[M - H]^-$ ions at 1057.8140 (calculated C60H114 O14: 1057.8136 Da) and 1083.8298 (calculated C62H116 O14: 1083.8292 Da), respectively; and the corresponding $[M + HCO_2]^-$ ions (Table s1e). HR MS^2 on the ion of *m/z* 1081 (Fig. 5a) gave rise to ions of *m/z* 841, arising from loss of $C_{15}H_{31}CHO$ (240 Da) by β-cleavage of mycolyl chain [23] to form a 6,6′-dipalmitoyl trehalose, and *m/z* 681, arising from cleavage of the α-1-O bond of the molecule to form a 6-14:0/18:0-mycolyl glucose (Scheme 5a; Table 5). The MS^3 spectrum of *m/z* 681 (1081 → 681; Fig. 5b) contained ions of *m/z* 621, 591 and 561 arising from rupture of the glucose ring (Scheme 5b), consistent with the notion that the mycolic acid substituent is located at 6 (or 6′) of the trehalose. Further dissociation of *m/z* 841 (1081 → 841; Fig. 5c) gave rise to the major ion at *m/z* 441, arising from cleavage of the α-1-O (or α′-1′-O) bond of the 6,6′-dihexadecanoyl trehalose, together with the *m/z* 585/603 ion pairs arising from loss of the 16:0-fatty acid substituent as ketene/FA. The MS^4 spectrum of the ion of *m/z* 441 (1081 → 841→ 441; Fig. 5d) contained ions of *m/z* 381 and 351 (Scheme 3c) arising from similar cleavages of the glucose ring as seen earlier (Scheme 5b), indicating that the 16:0-FA substituent is located at C6 (or 6′) of the trehalose. The realization of the 16:0-FA at C6 (or 6') is also consistent with observation of the analogous ions of *m/z* 407 and 377 in the MS^3 spectrum of *m/z* 467 (869 → 467), which arose from the $[M - H]^-$ ion of 6,6′-dioleory DAT standard at *m/z* 867 [24]. Thus, the above structural information clearly demonstrated the presence of 6-hexadecanoyl 6′-16:0/16:0-mycolyl trehalose (16:0-16:0/16:0-TMM). Similar MS^n approaches led to define the structure of *m/z* 1107.8, which is composed of 16:0-18:1/16:0-, 18:1-16:0/16:0-, and 16:0-18:0/16:1-TMM isomeric structures (Table s1e).

3.5. Characterization of other common lipid families from C. glutamicum and C. striatum

Both *C. glutamicum and C. striatum* belonging to the Corynebacteriaceae family are known to contain a good variety of lipids, including mycolic acids, triacylglycerol (TAG), phosphatidylglycerol (PG), cardiolipin (CL), phosphatidylinositol (PI), phosphatidylinositol mannoside (PIM), phosphatidylinositol dimmanoside (PIM2), acyl phosphatidylinositol mannoside (acyl-PIM), and trehalose dimycolate (TDM), in addition to the uncommon and some are minute lipids that were reported in this study earlier. Although the structures of these lipids have been described previously, the structure details such as the regiospecificity of the fatty acid substituents on the glycerol backbone (e.g., *Stereospecific Numbering; SN)* has been either undefined or mis-assigned [5,11]. Using LIT MS^n combined with high resolution mass spectrometry as previously reported, we redefine the structures including the regiospecificity of FA chain in the molecules, of the major species in each lipid classes including MA (Fig s3) [14], PG (Fig s4) [16], PI (Fig s5) [25], CL (Fig s6) [26], and TDM (Fig s7) [23] found in both *C. glutamicum and C. striatum* cells (supplemental materials Table s1 and s2).

4. Conclusions

In this study, we report the structures of the lipids extracted

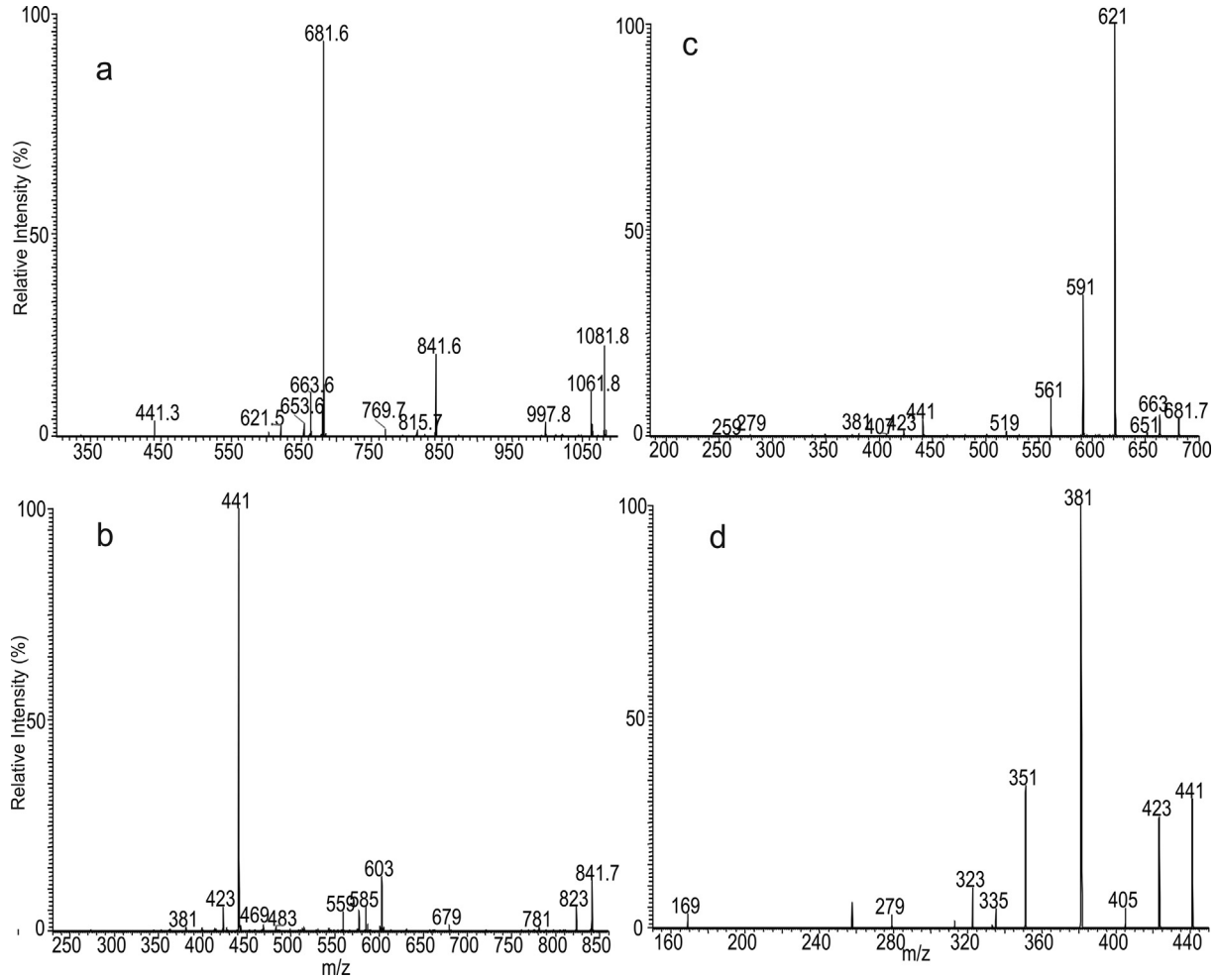

Fig. 5. The MS^2 spectrum of the ion of *m/z* 1081 (a), its MS^3 spectrum of the ion of *m/z* 681 (101 → 681)(b), MS^3 spectrum of the ion of *m/z* 841 (1081 → 841) (c), and MS^4 spectrum of the ion of *m/z* 441 (1081 → 841→ 441) (d).

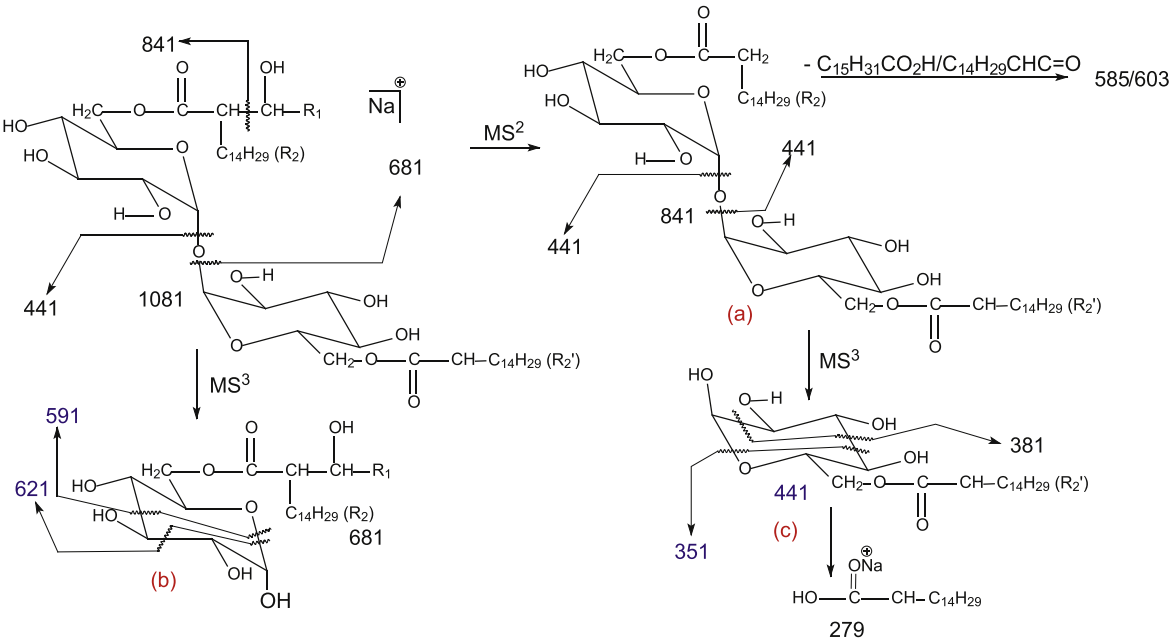

Scheme 5. The fragmentation processes proposed for the $[M + Na]^+$ ion of 6-palmitoyl 6'-(16:0/16:0)-mycolyl trehalose at m/z 1081. Further dissociation of ion m/z 841 (a) defines the 6,6'-diacyl trehalose structure, which is further confirmed by observation of the fragment ions from ring cleavages (b) and (c).

Please cite this article as: H.-Y.J. Wang et al., Unveiling the biodiversity of lipid species in *Corynebacteria*- characterization of the uncommon lipid families in *C. glutamicum* and pathogen *C. striatum* by mass spectrometry, Biochimie, https://doi.org/10.1016/j.biochi.2020.07.002

Table 5
High resolution MS^2 spectrum of the $[M + Na]^+$ ion of 6′-hexadecanoyl 6-mycolyl-trehalose at *m/z* 1081.

m/z	Rel. Intensity	Theo. Mass	Deviation	Composition	
Da	%	Da	mDa		ion structure
441.2822	1.69	441.2823	−0.12	C22H42 O7 Na	[16:0-acyl-Glc + Na]$^+$
621.5057	1.24	621.5065	−0.79	C36H70 O6 Na	681 - 2(CHOH)
663.5165	4.31	663.517	−0.5	C38H72 O7 Na	681 - H2O
681.5269	42.86	681.5276	−0.72	C38H74 O8 Na	[mycolyl-Glc + Na]$^+$
841.5643	8.56	841.5648	−0.44	C44H82 O13 Na	- C15H31CHO
1081.8095	9.44	1081.8101	−0.55	C60H114 O14 Na	[M+Na]$^+$

from *C. glutamicum* and in *C. striatum* cells, including several classes of uncommon lipid species and a new 1-mycolyl 2-acyl phosphatidylglycerol class. In addition to corynomycolic acid (16:0/16:0-MA), a hall mark of the *Corynebacterium* genus, we found that the mycolic acids in *C. glutamicum* are ranging from C26-C36 with one or two unsaturated bond mainly situated at the meromycolate branch, while in *C. striatum*, mycolic acids are ranging from C22-C34. The TDM family is abundant in both strains, but the chain length in *C. glutamicum* is significantly longer (supplemental Table s1 and s2). TAGs are abundant in *C. glutamicum*, but were not observed in *C. striatum*. However, we cannot exclude that the observed differences in the lipid profiles may be a reflection of the differences in the cell growth conditions and the lipid extraction method between the two strains.

The predominant species in each glycerolipid families found in this study all contained the 1-octadecenoyl, 2-hexadecanoyl glycerol core structure rather than the 1-hexadecanoyl, 2-octadecenoyl glycerol skeleton as previous reported for *Corynebacteria* [5,11,13]. This structural feature has been reported in the triacylglycerol and monomeromycolyl diacylglycerol lipid structures in M. smegmatis, where the 18:1- and 16:0-fatty acid substituents are exclusively located at *sn*-1 and *sn*-2, respectively [27]. *These findings are in accord with the knowledge that both* Mycobacterium *and Corynebacterium* belong to the suborder Corynebacterineae, and may share the same conserved machineries for lipid biosynthesis [28–31].

We revealed hundreds of lipid species in *C. glutamicum* and in *C. striatum* that evince the biodiversity of lipids in *Corynebacteria*, and further investigation in their biological roles maybe warranted.

Authors contribution

HYW, RVVT, NKG prepared the samples; FFH *conceived* the study, designed and performed the *experiments*; GD and FFH wrote the manuscript; All authors have approved the final article.

Declaration of competing interest

The authors declare no conflict of interest.

Acknowledgements

This work is supported by US Public Health Service Grants P41-GM103422 and P60-DK-20579.

Appendix A. Supplementary data

Supplementary data to this article can be found online at https://doi.org/10.1016/j.biochi.2020.07.002.

References

[1] A. Oliveira, L.C. Oliveira, F. Aburjaile, L. Benevides, S. Tiwari, S.B. Jamal, A. Silva, H.C.P. Figueiredo, P. Ghosh, R.W. Portela, V.A. De Carvalho Azevedo, A.R. Wattam, Insight of genus corynebacterium: ascertaining the role of pathogenic and non-pathogenic species, Front. Microbiol. 8 (2017).
[2] K. Bernard, The genus corynebacterium and other medically relevant coryneform-like bacteria, J. Clin. Microbiol. 50 (2012) 3152–3158.
[3] L. Martinez-Martinez, A.I. Suarez, J. Rodriguez-Bano, K. Bernard, M.A. Muniain, Clinical significance of Corynebacterium striatum isolated from human samples, Clin. Microbiol. Infect. 3 (1997) 634–639.
[4] Y. Otsuka, K. Ohkusu, Y. Kawamura, S. Baba, T. Ezaki, S. Kimura, Emergence of multidrug-resistant Corynebacterium striatum as a nosocomial pathogen in long-term hospitalized patients with underlying diseases, Diagn. Microbiol. Infect. Dis. 54 (2006) 109–114.
[5] N.K. Goldner, C. Bulow, K. Cho, M. Wallace, F.-F. Hsu, G.J. Patti, C.-A. Burnham, P. Schlesinger, G. Dantas, Mechanism of High-Level Daptomycin Resistance in *Corynebacterium Striatum*, 2018, p. 3, mSphere.
[6] S. Alibi, A. Ferjani, J. Boukadida, M.E. Cano, M. Fernandez-Martinez, L. Martinez-Martinez, J. Navas, Occurrence of Corynebacterium striatum as an emerging antibiotic-resistant nosocomial pathogen in a Tunisian hospital, Sci. Rep. 7 (2017) 17–10081.
[7] J.Y. Lee, Y.A. Na, E. Kim, H.S. Lee, P. Kim, The actinobacterium corynebacterium glutamicum, an industrial workhorse, J. Microbiol. Biotechnol. 26 (2016) 807–822.
[8] H. Marrakchi, M.-A. Lanéelle, M. Daffé, Mycolic acids: structures, biosynthesis, and beyond, Chem. Biol. 21 (2014) 67–85.
[9] L. Ott, E. Hacker, T. Kunert, I. Karrington, P. Etschel, R. Lang, V. Wiesmann, T. Wittenberg, A. Singh, C. Varela, A. Bhatt, V. Sangal, A. Burkovski, Analysis of Corynebacterium diphtheriae macrophage interaction: dispensability of corynomycolic acids for inhibition of phagolysosome maturation and identification of a new gene involved in synthesis of the corynomycolic acid layer, PloS One 12 (2017).
[10] G. Yagüe, M. Segovia, P.L. Valero-Guillén, Phospholipid composition of several clinically relevant Corynebacterium species as determined by mass spectrometry: an unusual fatty acyl moiety is present in inositol-containing phospholipids of Corynebacterium urealyticum, Microbiology 149 (2003) 1675–1685.
[11] S. Klatt, R. Brammananth, S. O'Callaghan, K.A. Kouremenos, D. Tull, P.K. Crellin, R.L. Coppel, M.J. McConville, Identification of novel lipid modifications and intermembrane dynamics in Corynebacterium glutamicum using high-resolution mass spectrometry, J. Lipid Res. 59 (2018) 1190–1204.
[12] E.G. Bligh, W.J. Dyer, A rapid method of total lipid extraction and purification, Can. J. Biochem. Physiol. 37 (1959) 911–917.
[13] R.V.V. Tatituri, P.A. Illarionov, L.G. Dover, J. Nigou, M. Gilleron, P. Hitchen, K. Krumbach, H.R. Morris, N. Spencer, A. Dell, L. Eggeling, G.S. Besra, Inactivation of corynebacterium glutamicum NCgl0452 and the role of MgtA in the biosynthesis of a novel mannosylated glycolipid involved in lipomannan biosynthesis, J. Biol. Chem. 282 (2007) 4561–4572.
[14] F.-F. Hsu, K. Soehl, J. Turk, A. Haas, Characterization of mycolic acids from the pathogen Rhodococcus equi by tandem mass spectrometry with electrospray ionization, Anal. Biochem. 409 (2011) 112–122.
[15] C. Huang, C. Freter, Lipid metabolism, apoptosis and cancer therapy, Int. J. Mol. Sci. 16 (2015) 924–949.
[16] F.-F. Hsu, J. Turk, Studies on phosphatidylglycerol with triple quadrupole tandem mass spectrometry with electrospray ionization: fragmentation processes and structural characterization, J. Am. Soc. Mass Spectrom. 12 (2001) 1036–1043.
[17] F.-F. Hsu, J. Turk, Electrospray ionization with low-energy collisionally activated dissociation tandem mass spectrometry of glycerophospholipids: mechanisms of fragmentation and structural characterization, J. Chromatogr. B 877 (2009) 2673–2695.
[18] F.-F. Hsu, J. Turk, Electrospray ionization multiple-stage linear ion-trap mass spectrometry for structural elucidation of triacylglycerols: assignment of fatty acyl groups on the glycerol backbone and location of double bonds, J. Am. Soc. Mass Spectrom. 21 (2010) 657–669.
[19] S.G. Wilkinson, Glycolipids containing glucose and uronic acids in Pseudomonas species, Biochim. Biophys. Acta 152 (1968) 227–229.
[20] S.G. Wilkinson, Lipids of Pseudomonas diminuta, Biochim. Biophys. Acta 187 (1969) 492–500.
[21] B.A. Wolucka, M.R. McNeil, L. Kalbe, C. Cocito, P.J. Brennan, Isolation and characterization of a novel glucuronosyl diacylglycerol from Mycobacterium smegmatis, Biochim. Biophys. Acta Lipids Lipid. Metabol. 1170 (1993) 131–136.

[22] F.-F. Hsu, J. Turk, Charge-driven fragmentation processes in diacyl glycerophosphatidic acids upon low-energy collisional activation. A mechanistic proposal, J. Am. Soc. Mass Spectrom. 11 (2000) 797–803.
[23] F.-F. Hsu, J. Wohlmann, J. Turk, A. Haas, Structural definition of trehalose 6-monomycolates and trehalose 6,6'-dimycolates from the pathogen rhodococcus equi by multiple-stage linear ion-trap mass spectrometry with electrospray ionization, J. Am. Soc. Mass Spectrom. 22 (2011) 2160–2170.
[24] C. Frankfater, R.B. Abramovitch, G.E. Purdy, J. Turk, L. Legentil, L. Lemiègre, F.-F. Hsu, Multiple-stage precursor ion separation and high resolution mass spectrometry toward structural characterization of 2,3-diacyltrehalose family from, Mycobact. Tubercul., Separ. 6 (2019) 4.
[25] F.-F. Hsu, J. Turk, Characterization of phosphatidylinositol, phosphatidylinositol-4-phosphate, and phosphatidylinositol-4,5-bisphosphate by electrospray ionization tandem mass spectrometry: a mechanistic study, J. Am. Soc. Mass Spectrom. 11 (2000) 986–999.
[26] F.-F. Hsu, J. Turk, E. Rhoades, D. Russell, Y. Shi, E. Groisman, Structural characterization of cardiolipin by tandem quadrupole and multiple-stage quadrupole ion-trap mass spectrometry with electrospray ionization, J. Am. Soc. Mass Spectrom. 16 (2005) 491–504.
[27] G. Purdy, S. Pacheco, J. Turk, F.-F. Hsu, Characterization of mycobacterial triacylglycerols and monomeromycolyl diacylglycerols from Mycobacterium smegmatis biofilm by electrospray ionization multiple-stage and high-resolution mass spectrometry, Anal. Bioanal. Chem. 405 (2013) 7415–7426.
[28] X. Liu, Y. Yin, J. Wu, Z. Liu, Structure and mechanism of an intramembrane liponucleotide synthetase central for phospholipid biosynthesis, Nat. Commun. 5 (2014).
[29] J.Y. Kiyasu, R.A. Pieringer, H. Paulus, E.P. Kennedy, The biosynthesis of phosphatidylglycerol, J. Biol. Chem. 238 (1963) 2293–2298.
[30] Y.-Y. Chang, E.P. Kennedy, Biosynthesis of phosphatidyl glycerophosphate in Escherichia coli, J. Lipid Res. 8 (1967) 447–455.
[31] J. Kanfer, E.P. Kennedy, Metabolism and function of bacterial lipids: II. Biosynthesis OF phospholipids IN ESCHERICHIA coli, J. Biol. Chem. 239 (1964) 1720–1726.

Please cite this article as: H.-Y.J. Wang et al., Unveiling the biodiversity of lipid species in *Corynebacteria*- characterization of the uncommon lipid families in *C. glutamicum* and pathogen *C. striatum* by mass spectrometry, Biochimie, https://doi.org/10.1016/j.biochi.2020.07.002